ELSEVIER

International Journal of Fatigue 24 (2002) 21–28

International Journal of Fatigue

www.elsevier.com/locate/ijfatigue

Fatigue assessment of an electrical resistance welded oil pipeline

M.D. Chapetti [a], J.L. Otegui [a,*], J. Motylicki [b]

[a] *INTEMA, Welding and Fracture Division, University of Mar del Plata, Mar del Plata, Argentina*
[b] *OLDELVAL S.A., Gral. Roca, Rio Negro, Argentina*

Received 11 November 1999; received in revised form 1 June 2001; accepted 20 July 2001

Abstract

A blowout in a 14 in. diameter, 1/4 in. thick API 5L X46 oil pipeline was due to the sudden propagation of a fracture at the longitudinal Electrical Resistance Welding (ERW) weld. The cracks initiated from small hook crack-type defects on the external surface of the tube, in the highly deformed and hardened central area of the ERW weld. Fatigue tests were carried out to characterize initiation and propagation of fatigue cracks in base and weld metals, in two regions of the pipeline. Specimens were subjected to cyclic stresses similar to those that were produced during the passage of the scraper. The fatigue growth was modeled by integrating experimental results. Predicted fatigue lives of about 20,000 cycles justify fatigue propagation up to failure in weld metal, from initial 2 mm deep defects introduced during manufacturing.

Keywords: Fatigue assessment; Electrical Resistance Welding (ERW); Oil pipeline

1. Introduction

In 1998, an oil pipeline company faced a blowout in a 20 year old 14 in. diameter, 1/4 in. thick pipe, due to the sudden propagation of a preexisting longitudinal crack at the outer surface of the Electrical Resistance Welding (ERW) longitudinal weld, see Fig. 1 [1]. The total length of the fracture was 480 cm. The blowout occurred 40 min after the passage of the scraper through the section, 950 m downstream from a pumping station. Due to the resulting abrupt fall of pressure, the scraper returned back and stopped in the middle of the fractured area. The square windows observed in Fig. 1 were cut in order to take the remnant oil out of the line and to extract the scraper.

Visual inspection revealed the presence of a surface crack, with a depth of the order of 70% of the thickness, and a length of about 160 mm, whose sudden brittle propagation provoked the blowout. The inspected surfaces were corroded due to a long exposition to weather conditions before the examination. Surfaces had to be cleaned with diluted hydrochloric acid, but it was not possible to recover many details of the propagation history in the surfaces. The crack shows signs of propagation and coalescence of individual defects starting from the external surface, with variable surface lengths between 10 and 40 mm. Fig. 2(a) shows the crack surface, while Fig. 3(b) shows a sketch of what is seen in Fig. 2(a). Arrows indicate initiation sites on the outer pipe surface, and sense of growth on the crack surface. Beach marks indicating the shape of successive crack fronts during propagation, coalescence stages and final crack size before the blowout can be noted.

Fatigue behavior of line pipes with defects has become a major concern because of large daily pressure fluctuations. The design codes for fatigue of structures are based on *S–N* curves determined experimentally, and classify the design details in specific ranges of severity [2]. This analysis method is based on the determination from the total fatigue life of a component, up to its failure, and it does not consider the different phases of the process: (a) nucleation of microscopic cracks and coalescence to form a detectable defect; (b) subsequent propagation of this defect (crack growth); and (c) failure or final instability. Small fabrication defects in the longitudinal welds, such as surface roughness, scratches or inclusions can act as initial cracks, for what the 'initiation' stage can be short.

Fatigue initiation of cracks is characterized by *S–N*

* Corresponding author. Tel.: +54-223-481-6600; fax: +54-223-481-0046.
E-mail address: jotegui@fi.mdp.edu.ar (J.L. Otegui).

0142-1123/01/$ - see front matter
PII: S0142-1123(01)00111-6

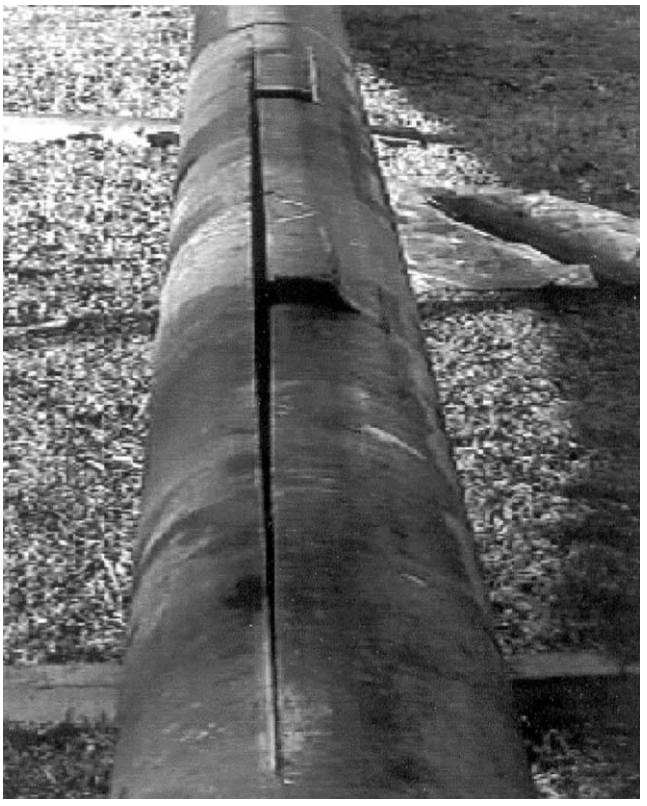

Fig. 1. Sudden propagation of a longitudinal crack at the outer surface of the ERW seam weld. Note windows made to recover oil.

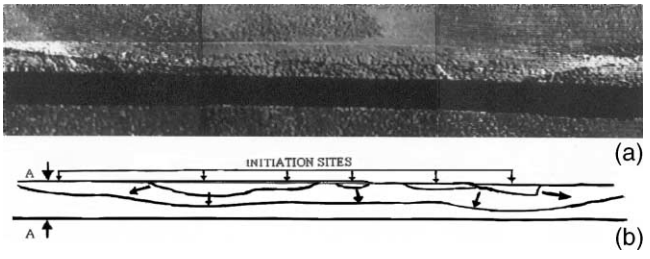

Fig. 2. (a) Surface of initiating crack, showing signs of fatigue growth. (b) A sketch of what is seen. Arrows indicate initiation sites and sense of growth.

curves that associate the applied cyclic stress amplitude (ΔS) with the number of cycles until the detection of cracks (N) [3,4]. To characterize fatigue crack propagation, linear elastic fracture mechanics (LEFM) associates the applied amplitude of stress intensity factor (ΔK) with crack propagation rates (da/dn), [5,6]. The so called Region II can often be represented by the simple form attributed to Paris et al: $da/dn=C\Delta K^m$, where $\Delta K=K_{max}-K_{min}$, these referring to the maximum ad minimum values of the stress intensity factors in any given load cycle [7].

Longitudinal welds generate stress raisers, residual stresses and metallurgical changes. Transverse residual stresses are about half the yield strength of the base material. Defects typically associated to ERWs, especially to those welds carried out at low frequency, are due to incomplete joining and internal defects (inclusions, lacks of fusion, etc.) in the middle area of the weld [8]. During the weld process the heated material is ejected from the center of the thickness toward the surfaces of the pipe. Lamination defects, originally parallel to the surface, are reoriented through the thickness. This decreases the resistance of the weld to circumferential stresses. The ejected material is eliminated mechanically, and this process leaves marks in the surfaces that work as possible crack initiation areas. One typical form of defect is the so called hook crack, in which a curved crack is formed a couple of mm away from the weld centerline, following the lamination planes [9].

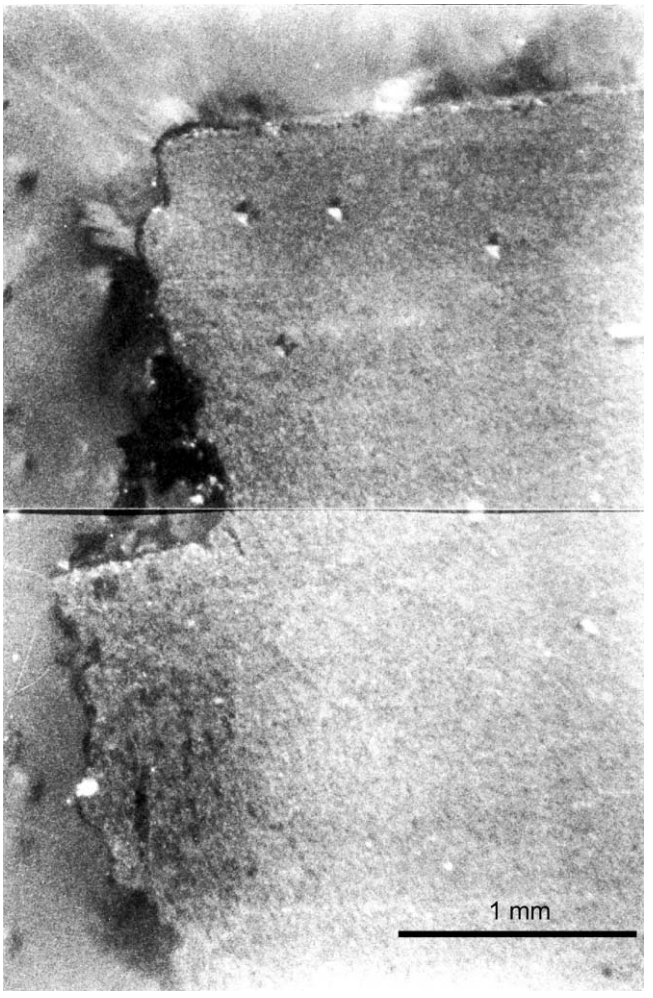

Fig. 3. Cross-section of the first 3 millimeter of the crack path (×30).

One of the major concerns in maintaining pipeline integrity is third-party mechanical damage caused by outside forces resulting in defects. Most of the previous research work has been concentrated on the complex behavior of a gouge within a dent, the most typical and also severest form of mechanical damage in the industry [10,11].

Fatigue tests for line pipes with a gouge in a dent were

Table 1
Chemical composition

Tube	C (%)	Mn (%)	P (%)	S (%)	Si (%)
1	0.13	0.75	0.03	0.03	0.11
2	0.19	0.69	0.02	0.04	0.12
3	0.24	1.08	0.02	0.03	0.06

carried out by several authors [12,13]. Using line pipes with a relatively mild artificial gouge (0–30% of wall thickness) in dent (10% of pipe diameter) type defect, Hagiwara et al. [14] suggested an equation for estimating the fatigue life, N_f, as a function of the hoop stress amplitude, $\Delta\sigma$:

$$N_f = C(d/D)^{\alpha}(t/T)^{\beta}(\Delta\sigma/E)^{\gamma}$$

where E is Young's modulus, and C, α, β, and γ are regression coefficients. $\Delta\sigma/E$ means the elastic strain range. Experimental fatigue test results N_f were found to be in good agreement with N_f.

Although useful for predictions in a pipeline with a mild defect, this equation has not been shown to be applicable to a pipeline with a more severe defect. ERW line pipes generally also have large residual stresses. The effects of residual stress of ERW line pipes on fatigue behavior with a severe artificial defect was examined in fatigue tests carried out by Hagiwara et al. [15] on 20–30 cm diameter line pipes. By the parameter Q, a function of defect size and fracture toughness, fatigue behavior could be explained well. Fatigue behavior differed above and below the threshold value of Q (Q_{th}). When $Q<Q_{th}$ crack propagation was initially associated with ductile crack growth, and therefore fatigue life N_f decreased to less than 1000 cycles. On the contrary, N_f was larger than 1000 cycles when $Q>Q_{th}$. N_f was predictable with a power law equation incorporating dent depth, gouge depth and stress amplitude when $Q>Q_{th}$. A gouge in a dent with $Q<Q_{th}$ requires immediate repair or replacement.

2. Failure analysis

Chemical and mechanical properties of the materials involved in the failure are shown in Tables 1 and 2. Tube material complies with the requirements of API 5L X46 standard [1]. Hardness and microhardeness Vickers tests of base and weld metals show low hardness in base material (20 HRC) that allow us to discard susceptibility to hydrogen enbrittlement, possibly generated by cathodic overprotection. In the central area of the longitudinal welds an increase of hardness is reported up to 30 HRC, making the welds marginally susceptible to hydrogen enbrittlement. This higher hardness coincides with a change in microstructural characteristics, which is ferritic pearlitic in base metal and lower bainitic or martensitic in the highly deformed area of the weld centerline. It also coincides with a higher strength and lower ductility (see Table 2). The intermediate areas present ferritic bainitic microstructures.

Extensive magnetic particle tests in tracts of pipe adjacent to the failed tubes failed to detect any cracks. Indications in weld material have been associated to shallow longitudinal marks produced by the machining of the weld reinforcement. It is apparent from the evolution of the cracks that there were at least three or four initiation sites. Cross-sections of the cracked weld were made, in order to find indications of these initial cracks. As an example, Fig. 3 (×30) shows the first three millimeters of the crack path along the cross-section indicated as AA in Fig. 2(b). The crack path is clearly influenced by the microstructure, which forces 90 degree changes as seen in the top left and middle of the figure. This second, larger kink corresponds to the onset of the final unstable fracture.

SEM fractographic evaluations show a clear differentiation between the smooth fatigue crack surfaces and the rough surface of the final fracture, see Fig. 4 (×10). The surface of the final fracture shows parallel bands which correlate with the microstructural banding produced during lamination of the pipe. Fig. 4 also shows that in the mid-section of the longitudinal welds there are two-dimensional or volumetric discontinuities, aligned longitudinally and in the sense of the thickness. They are due to small defects of lack of fusion, with caught non-metallic inclusions, located in the highly deformed weld area. They present plane or curved surfaces, with small protuberances in the ends. Maximum depths and lengths measured are less than 0.5 mm, while most defects are about 0.25 mm.

Experimentally determined fracture toughness of base

Table 2
Tensile properties and fracture toughness (L: longitudinal, C: circumferential)

Tube material	Sy (MPa		UTS (MPa)		Elong (%)		Reduc (%)		K_{1C} (MPa m$^{1/2}$)
	L	C	L	C	L	C	L	C	C
BASE	425	489	532	556	28	16	60	41	44
WELD	593		721		23		48		37

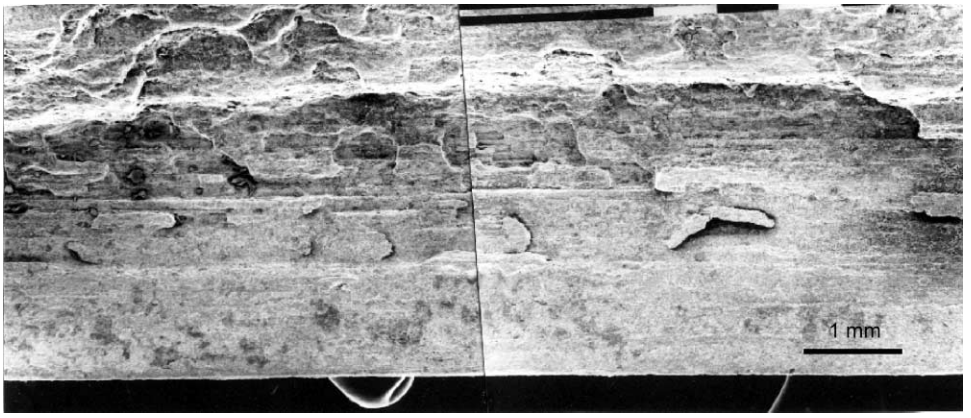

Fig. 4. SEM fractography (×10), showing surfaces of fatigue crack and final fracture.

and weld materials involved in the failure is very low, of the order of 40 MPa $m^{1/2}$, see Table 2. With these results a flaw criticity assessment was carried out [4]. The maximum acceptable depth of an external surface defect on the weld that will not cause fracture is about 4.5 mm. This parameter allowed us to verify an appropriate correspondence with the size of the fatigue crack when the blowout occurred. It also allows us to define the required sensitivity for future non-destructive evaluations in order to prevent this kind of failure.

This study established that in-service propagation of the cracks, as shown in Fig. 2, took place at the mid section of the ERW seam weld of the pipe by a mechanism of fatigue. These cracks propagated from small surface cracks or defects, located at the bottom of the longitudinal machining marks on the outer surface of the tube, in the highly deformed and hardened central area of the ERW longitudinal weld (see Fig. 1). In order to identify a mechanism of crack initiation or the shape and size of preexisting defects, extensive fractographic analyses were done on samples taken from other positions of the pipeline. Where In Line Inspection (ILI) had revealed the probable existence of crack like defects, samples were cut out of the pipeline and inspected. As expected, several hook cracks were found, but their morphology varied from defect to defect. Two extreme examples are presented in Figs. 5 and 6.

Fig. 5 (×5) shows a cross-section of the weld, in which a large hook crack is seen. This is a volumetric defect, with its innermost portion oriented parallel to the pipe

Fig. 5. A benign type of hook crack in the ERW (×5).

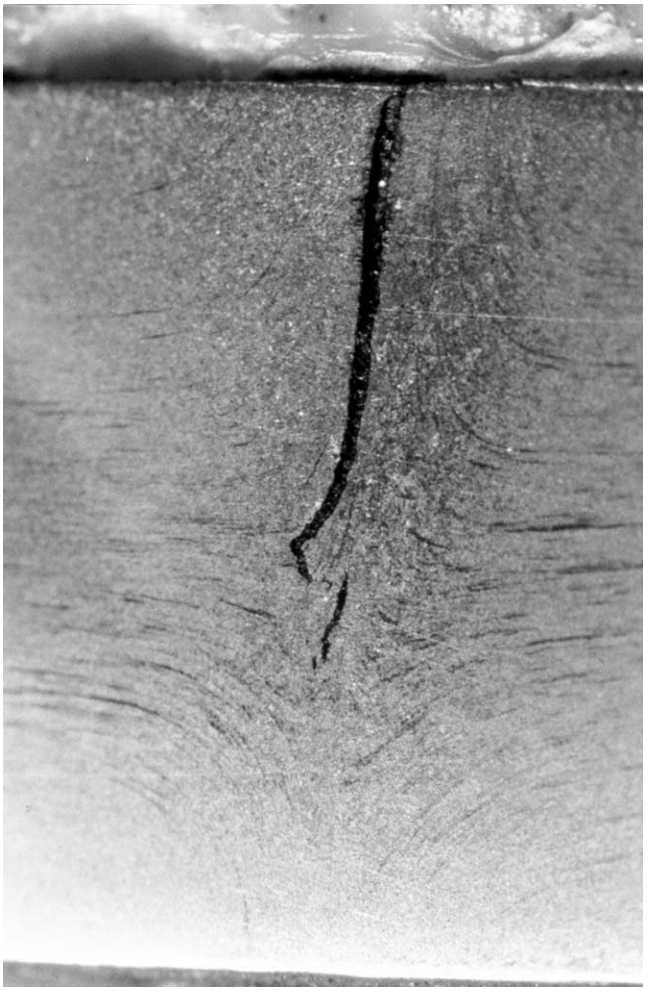

Fig. 6. A sharp, through the thickness hook crack in the ERW (×20).

surface. The crack driving force in its tip is quite small, since hoop stresses are almost parallel to the crack surface. This is the most benign type of hook crack, the most frequently found in field, and the most widely discussed in the literature. Experimental tensile test results verified that its significance on the strength of the pipe is related to the reduced load carrying ligament.

The polished and etched cross-section of Fig. 6 (×20) shows a different type of hook crack. The main crack breaks the outer surface (upper part of the figure) and is very sharp. The crack path tends to follow the microstracutrual banding, right up to the mid thickness. Near the crack tip of this main crack, other small cracks are seen, related to the banding of the material f1owing into the inner surface. The figure shows how interaction among all these cracks can give rise to a rather deep, sharp and through thickness crack. This defect is an indication of the probable source of the original defect that leads to the fatigue failure under study. Fatigue propagation from the initial defect was related to cyclic loads originated in changes of pressure in the tube. Such pressure changes existed indeed during most of the service life of the pipe. Pressure changes of large amplitude and low frequency are associated to the maneuvers for the passage of the scraper.

To eliminate the paraffin deposits and to improve the efficiency of the transport, the scraper is regularly passed through this section. Until the occurrence of this failure, the compressor plant did not possess a scraper trap. Therefore, in every passage of the scraper suction discharge pressures had to be balanced. Discharge pressure was decreased from 70 to 40 kg/cm^2, and suction pressure increased from 7 to 40 kg/cm^2. The pressures in other compressor plants along the line had also to be adjusted during these maneuvers, but in these cases the decrease in the discharge pressure was only from 70 to 63 kg/cm^2, while the increase in suction pressure was from 7 to 25 kg/cm^2. During the last 5 years, the scraper was passed once a week in winter and twice a week in summer, but data on the frequency during the previous 30 years of service is not reliable. Installation of scraper traps has already been finished in all plants.

It is interesting to determine how well the failure could have been predicted by existing modeling tools. As mentioned in Section 1, Hagiwara et al. [15] proposed using the parameter Q, a function of defect size and fracture toughness incorporating dent depth, gouge depth and stress amplitude, to explain fatigue behavior. When $Q<Q_{th}$ fatigue life N_f is less than 1000 cycles, and requires immediate repair or replacement. Q_{th} has been experimentally defined at about 10,000 N. Considering the low toughness of the Salitral weld metal, and the large original crack depth (approximately t=2 mm, $2c$=20 mm), Q could probably be well below Q_{th}. To obtain $Q=Q_{th}$ it is required that d=10 mm, a defect one order of magnitude larger than the scratch sizes found in the ERW welds being evaluated.

The studied failure defined the convenience of defining acceptable maximum limits to the frequency of pressure cycles in the pipes, and evaluating the conditions of defect criticity in the longitudinal welds, the methodologies for non-destructive inspection of possible longitudinal defects, and the fatigue initiation and propagation behavior of surface defects, especially in weld material.

3. Experimental fatigue evaluation

It can be expected that for a given level of applied cyclic stresses the weld material would present a smaller initiation life than the base material. This effect is due to the different surface conditions. Similarly, it can be expected that crack propagation results could allow us to detect differences in fatigue crack propagation rates, due to the differences in microstructure between both materials and also because of the presence of small inclusions and other weld metal defects, that probably increase the average propagation rate. Fatigue tests [17] were carried out to characterize initiation and propagation of fatigue cracks in base and weld metals from two different sites of the pipeline, called Allen and Salitral. These tracts have different ERW longitudinal welds, made by different manufacturers. Specimens were subjected to cyclic stresses similar to those that were produced during the maneuvres of passage of the scraper. Fatigue samples at Salitral were extracted from pipeline tracts contiguous to the failed part, whose surfaces remained intact.

Straightening of the samples was made according to BS7448 Part 2 [16], ‘gull wing’ type test tube. Three point bending tests were carried out in a soft ‘walking beam’ type deformation controlled fatigue testing machine, at a frequency of 10 Hz. Initiation tests were carried out from natural surface defects at the external surface wall of the welds. Semielliptic surface 0.4 mm deep initiation notches were machined in the propagation specimens in the longitudinal direction [18]. To define the initiation S–N Wöhler curves, the period of initiation was defined as the number of cycles necessary to develop a crack 1 mm deep, and therefore involves the periods of microcrack initiation and coalescence. As discussed in a previous paper [20], it is approximately at this stage that the first crack coalescence from randomly distributed surface defects is completed, and the crack front leaves the notch plastic zone at geometric stress raisers in the surface of the weld. For the fatigue crack propagation tests, the minimum stress was kept at 60 MPa, to maintain the maximum stress below the fracture stress.

Ink marking was used to obtain indications of crack development. Ink marks were observed ‘post-mortem’ with a traveling microscope. Multiple strain gauges were applied near the probable initiation sites and the machined notches, to detect variations in compliance arising from crack initiation and early growth. One strip

containing four 2.1 mm long strain gauges were bonded to the plate surface, about 2.5 mm from the crack plane. Details of this monitoring technique are given elsewhere [19]. The strain gauge monitoring system gave very reasonable predictions of crack sizes and shapes, for depths ranging from 0.2 to 3 mm. For all tests, 'failure' was defined as a crack depth of the order of 4 mm, since only a few additional cycles were generally required to develop a through-thickness crack from this point.

The analysis of the initiation and propagation of cracks, and their interactions with microstructure and defects, was carried out with optical (10×–1000×), and electronic scanning microscopy. Multiple crack initiation was found within the longitudinal marks at the surfaces of the welds in both materials.

The propagated fatigue cracks followed a trajectory mostly perpendicular to the applied stress, but were sometimes forced to follow a curved and stepped path, as shown in the cross-section of Fig. 7 (Salitral, ×80), and in greater detail again in Fig. 8 (same specimen, ×400). It can be seen that this path is induced by the microstructural banding in this highly deformed region of the ERW seam weld, and possibly favored by the high through the thickness stress gradient generated by the three point bending load in the small thickness specimens (6.35 mm). In a membrane stress distribution this stepped crack behavior could be not so marked.

Fig. 7. Trajectory of propagated fatigue cracks. Cross-section of Salitral sample (×80).

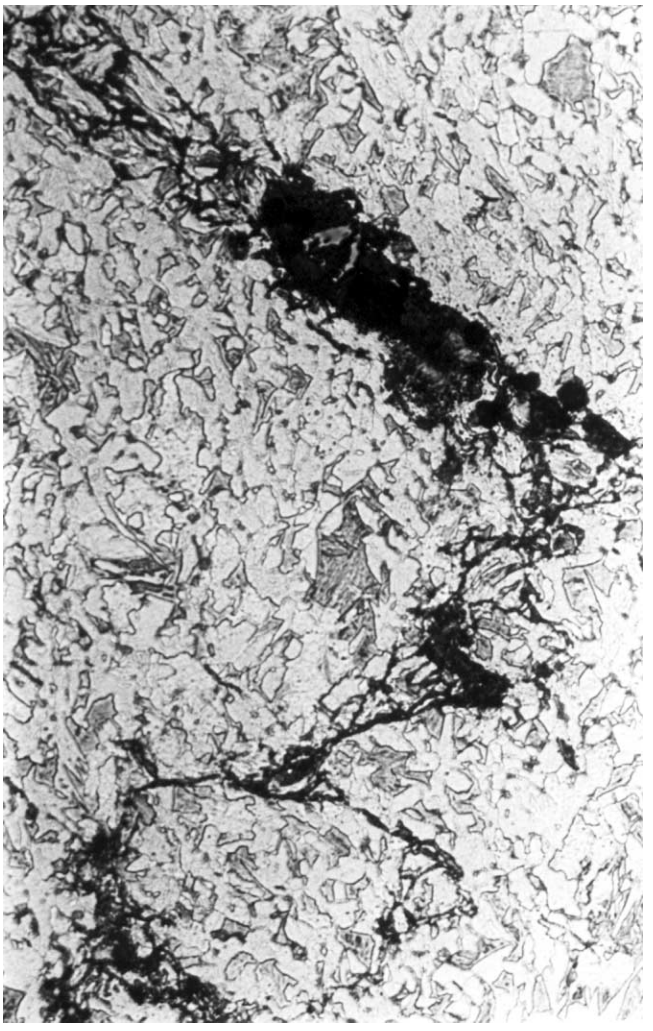

Fig. 8. Stepped path induced by microstructural banding in the ERW metal. Cross-section of Salitral sample (×400).

Fig. 9 shows the *S–N* curves for fatigue initiation from the outer surface of pipe base metal and seam welds. It can be seen that the number of cycles to initiation of fatigue cracks is relatively high in all cases, and especially in the base material. For 230 MPa stress cycles, which represent those developed during pressure variations from zero to the maximum pressure of the pipeline, the number of cycles necessary to initiate a crack is between 100,000 and 200,000 for the weld material, and about 500,000 for base metal. In the Salitral weld tests, initiation is located in defects within a microstructure with low resistance, mostly non-metallic inclusions located in the surface, in the weld center line. Cracks grow straight, following the direction defined by

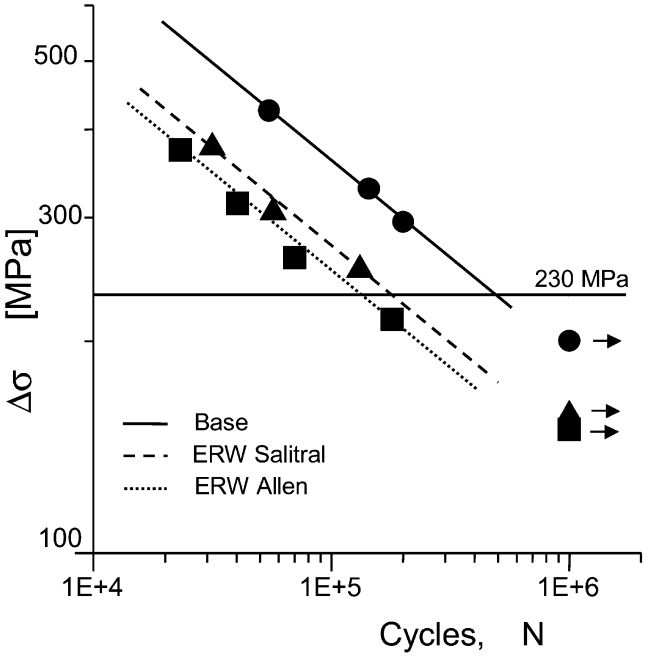

Fig. 9. *S–N* curves for fatigue initiation from the outer surface of the pipe base metal and seam welds.

the applied ΔK, until a depth of around 1 mm, when the stepped growth pattern starts. Crack propagation is transgranular, following the alignment of the largest ferritic areas. In the Allen weld tests, the cracks start from inclusions aligned along surface stress raisers, at the bottom of a step produced by a mismatch of the post welding shaving process. In this area the microstructure does not present important banding, for which the crack always grows in the direction of largest applied ΔK. As an example, Fig. 10 shows the experimental da/dN vs. ΔK values for the ERW metal at Salitral, from which the fatigue constants C and m were derived.

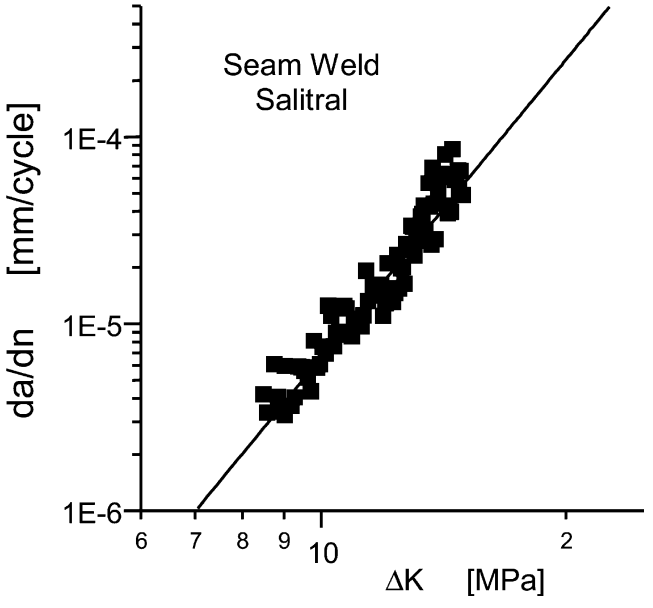

Fig. 10. Experimental fatigue crack growth data for the EMW metal at Salitral.

4. Discussion of results

The development of crack aspect ratios (length to depth, a/c) is an important factor in fracture mechanics analyses of fatigue life [20]. Large-crack values of a/c after final coalescence are in general determined by the geometry of the original defects and the marks at the weld surface. The failure analysis showed that the different small cracks initiated at the surface of the longitudinal weld coalesced relatively early, allowing the development of only one macrocrack with a small aspect ratio. The small cracks coalesced in periodic groups, giving rise to mismatched macrocracks with an additional coalescence stage. This additional coalescence stage occurs at different crack depths, depending on the mismatch between the planes of neighboring cracks and mainly on the angle between their surface tips [20]. In this case, the mismatch is small, and therefore crack coalescence in these regions is accelerated, increasing stress-raising interactions between neighboring cracks and increasing crack propagation rates.

For an initial defect depth of 0.6 mm and an applied stress range of 97 Mpa, which is the hoop stress generated by the passage of the scraper, applied ΔK is about 4.21 Mpa $m^{1/2}$, similar to the propagation threshold. Therefore, it is not very probable that a flaw less than 1 mm deep could propagate solely by fatigue. At this stress level the initial defect should have been much deeper than 1 mm. Otherwise, considerable larger stress cycles should have occurred to propagate the cracks. Although some of these cycles were produced during the total elimination of the pressure in the pipes, these were very few during service life.

Table 3 shows the experimentally determined fatigue constants C and m. Note that Paris m exponents are very high. This is probably because tests were carried out with ΔK values relatively low, near the propagation threshold. Fatigue growth of cracks from initial depths of 0.6 mm up to a final depth of 4.5 mm, was modeled by integrating the experimental results, considering a single crack. Large fatigue lives were obtained, as shown in Table 3. Real service life of the pipe was only 20 years. The largest inclusion found in the propagation pattern within the fatigue tests was 0.2 mm long. This is much smaller than the largest inclusion found in the fracture surfaces of the blowout, which were about 2 mm long (see Fig. 4). These defects can considerably increase the propagation rates of the cracks.

When the initiation is multiple, coalescence processes are obtained that could increase growth rates. This was indeed observed in the crack that led to the blowout. In

Table 3
Experimental fatigue constants C and m, and number of necessary cycles to grow a crack from an initial depth a_0 up to the critical size, a_f=4.5 mm

Material	m	C (mm/cycle)	Number of cycles, $N(\Delta\sigma$=97 MPa)		
			a_0=0.6 mm	a_0=1.2 mm	a_0=2 mm
Base	6	3.818×10^{-12}	25,500,000	563,000	33,500
Weld Salitral	5.29	3.327×10^{-11}	7,950,000	287,000	24,400
Weld Allen	5.27	4.7×10^{-11}	5,790,000	212,000	18,200

a multiple crack initiation process propagation rates can increase, if multiple cracks are mostly coplanar [20]. In these conditions, fatigue estimations from 2 mm deep defects yielded total propagation lives of 18,000 cycles in the case of Allen and 24,000 cycles in the case of Salitral. These estimated life cycles justify fatigue propagation up to failure in weld metal. Therefore, it is concluded that preexisting cracks related to hook cracks or other weld defects, grew by fatigue during service, generating a critical longitudinal crack that the lead to the blowout of the pipeline.

5. Conclusions

A blowout in a 14 in. diameter, 1/4 in. thick API 5L X46 oil pipeline was due to the sudden propagation of a fracture at the longitudinal ERW weld. Fractographic, microstructural, chemical and mechanical analyses were carried out. The lower bainitic or martensitic weld metal, with hardness of 30 HRC, is marginally susceptible to hydrogen enbrittlement. Crack propagation took place by fatigue. The fatigue crack initiated from a hook crack on the external surface of the tube, in the highly deformed and hardened central area of the ERW weld. Fatigue tests were carried out to characterize initiation and propagation of fatigue cracks in base and weld metals, in two regions of the pipeline. Specimens were subjected to cyclic stresses similar to those that were produced during the passage of the scraper, twice a week during many years. The fatigue growth was modeled by integrating experimental results. Predicted fatigue lives of about 20,000 cycles justify fatigue propagation up to failure in weld metal, from initial 2 mm deep defects.

Acknowledgements

This research work was partially funded by CONICET (Consejo Nacional de Investigaciones Científicas y Técnicas de la República Argentina), by Agencia Nacional de Promocion Cientifica de la Republica Argentina (PICTs 12-04585 and 12-04586), and by OLDELVAL S.A.

References

[1] Report GIE 20-09/98//22-10/98. Análisis de Fallas en Linea 1, Allen y Salitral de la Vidriera, e Indicaciones en Linea 2, Allen, 1998.
[2] Barsom J, Rolfe S. Fracture and fatigue control in structures. 2nd ed. Englewood Cliffs (NJ): Prentice-Hall; 1987.
[3] Gurney TA. Fatigue of welded structures. Cambridge (MA): Cambridge University Press; 1978.
[4] BSI PD6493/91. Guidance on some methods for assessing the acceptability of flaws in fusion welded structures. British Standards Institution, 1991.
[5] Broek D. Practical use of fractrure mechanics. Dordrecht: Kluwer Academic Publishers; 1990.
[6] Anderson TL. Fracture mechanics, fundamentals and applications. 2nd ed. Boca Raton (FL): CRC Press; 1995.
[7] Fuchs HO. Metal fatigue in engineering, 1980.
[8] American Welding Society. Welding handbook. Miami: American Welding Society; 1995.
[9] Kiefner F et al. Failure analysis of pipelines, ASM handbook. ASM International, 1997.
[10] Maxey WA. Outside force defect behavior. In: 7th Symposium on Line Pipe Research, American Gas Association, 14, 1996:1–33.
[11] Mayfield ME, Maxey WA, Wilkowski CTM. Fracture initiation tolerance of line pipe. In: Sixth Symposium of Line Pipe Research, American Gas Association, F1, 1979.
[12] Fowler JR, Alexander CR, Kovach PJ, Connelly LM. Fatigue life of pipelines with dents and gouges subjected to cyclic internal pressure. Pipeline Eng ASME, PD-Vol 69:17–35, 1995.
[13] Kiefner JF, Alexander CR, Fowler JR. Repair of dents containing minor scratches. In: 9th Symposium on Pipeline Research, PRC International, American Gas Association, 1996.
[14] Hagiwara N, Mejiere Y, Oguchi N, Zarea M, Charnpavere R. Study on the fatigue behaviour of steel pipes containing idealized flaws under fluctuating pressure. In: International Gas Research Conference (IGRC'98), San Diego (CA, USA); American Gas Association, 1998.
[15] Hagiwara N, Oguchi H. Fatigue behaviour of line pipes subjected to severe mechanical damage. In: International Pipeline Conference — vol. 1. New York: ASME, 1998.
[16] BSI BS7448 Part 2. British Standards Institution.
[17] American Society for Testing of Materials. ASTM E647, Standard test method for measurement of fatigue crack growth rates, 1988.
[18] Newman JC, Raju IS. An empirical stress intensity factor equation for the surface crack. Engng Fract Mech 1981;15(12):185–92.
[19] Otegui JL, Mohaupth UH, Burns DJ. A strain gauge technique for monitoring small fatigue cracks in welds. Eng Fract Mech 1991;40(3):549–70.
[20] Chapetti MD, Otegui JL. Importance of toe irregularity for fatigue resistance of automatic welds. Int J Fatigue 1995;17(8):531–8.